A Digalla[1.1]ferrocenophane and Its Coordination Chemistry: Synthesis and Structure of [{Fe(η^5-C_5H_4)$_2$}$_2${GaMe}$_2$] and of the Adducts [{Fe(η^5-C_5H_4)$_2$}$_2${GaMe(D)}$_2$] (D = Monodentate Donor) and [{Fe(η^5-C_5H_4)$_2$}$_2${GaMe}$_2$D] (D = Bidentate Donor)

Alexander Althoff, Peter Jutzi,* Norman Lenze, Beate Neumann, Anja Stammler, and Hans-Georg Stammler

Fakultät für Chemie, Universität Bielefeld, 33615 Bielefeld, Germany

Received February 20, 2003

Gentle warming of 1,1′-bis(dimethylgallyl)ferrocene (**1**) leads to the formation of trimethylgallium and the thermolabile compound [{Fe(η^5-C_5H_4)$_2$}$_2${GaMe}$_2$] (**2**), a [1.1]ferrocenophane featuring group 13 elements in bridging positions. While NMR data for **2** prove a dynamic structure in solution, X-ray data reveal an anti conformation of the ferrocenophane framework in the solid state. The anti conformation is maintained in the thermolabile adducts **2a**−**g**, which are obtained from **2** and the donors diethyl ether (**2a**), pyridine (**2b**), pyrimidine (**2c**), quinoxaline (**2d**), DMSO (**2e**), pyrazine (**2f**), and dioxane (**2g**), by donor-exchange reactions (**2b**−**g**) or on gentle warming of the respective donor adducts of **1**. Rodlike polymers are formed either by interaction of **2** with bidentate donors (**2f**,**g**) or by π-stacking effects of aromatic molecules acting as monodentate donors (**2b**−**d**). Steric requirements inhibit the complex formation between **2** and the donor phenazine. A cyclic voltammogram of **2b** in pyridine reveals two reversible oxidation steps at −314 and −114 mV, indicating only weak electron delocalization in the cationic species. The formation of **2** from **1** has been shown to be reversible and thus is an example of an application of "dynamic covalent chemistry" as synthetic strategy.

Introduction

One of the rich areas of metallocene chemistry is that of ferrocenophanes. Particularly interesting are those compounds in which the ferrocene units are fixed in a mutually coplanar geometry. This criterion is met ideally by the binuclear [*m.m*]ferrocenophanes [0.0]-ferrocenophane ([Fe(C_5H_4)$_2$]$_2$) and [2.2]ferrocenophane-1,13-diyne ([{Fe(C_5H_4)$_2$}$_2$(C≡C)$_2$]) and to a lesser extent by the [1.1]ferrocenophanes [{Fe(C_5H_4)$_2$}$_2$(CR_2)$_2$].[1,2] Until recently only a few heteroatom-bridged compounds [{Fe(C_5H_4)$_2$}$_2$$X_2$] (X = $SiMe_2$, $SnBu_2$, $PbPh_2$, PMen; Men = menthyl) have been reported. They contain group 14 or 15 atoms at the 1- and 12-positions.[3]

Recently we reported on the novel trinuclear ferrocenophane [{Fe(C_5H_4)$_2$}$_3${Ga(C_5H_5N)}$_2$], which was formed in a highly selective reaction by heating a solution of 1,1′-bis(dimethylgallyl)ferrocene (**1**) in toluene/pyridine.[4] In the reaction sequence, the digalla[1.1]-ferrocenophane [{Fe(C_5H_4)$_2$}$_2${GaMe(C_5H_5N)}$_2$] (**2b**) is an intermediate, which then goes on to form [{Fe(C_5H_4)$_2$}$_3${Ga(C_5H_5N)}$_2$]. **2b** is the first group 13 bridged [1.1]ferrocenophane. Shortly after publication of the synthesis of **2b** another digalla[1.1]ferrocenophane, namely the compound [{Fe(C_5H_4)$_2$}$_2${GaCH($SiMe_3$)$_2$}$_2$], has been reported.[5]

The favorable electrochemical properties make ferrocene fragments especially promising candidates for incorporation into the backbone of polymeric compounds. Such materials have been shown to possess interesting electrical, magnetic, and optical properties as a result of electron delocalization.[6] One route to polyferrocenyl species is based on the formation of donor−acceptor bonds between difunctional nitrogen bases and Fe(η^5-$C_5H_4EMe_2$)$_2$ (E = B, Ga) units. Among these substances, the compounds [Fe(η^5-$C_5H_4GaMe_2$)$_2$L]$_n$ (L = phenazine)[7] and [Fe(η^5-$C_5H_4BMe_2$)$_2$L]$_n$ (L = 4,4′-bipyridyl, pyrazine)[8] have been structurally characterized.

In the present paper, we report in more detail on the synthesis and structure of the digallaferrocenophane−pyridine adduct **2b**, of further adducts (**2a**,**c**−**g**), and of

(1) For metal−metal interactions in linked metallocenes see: Barlow, S.; O'Hare, D. *Chem. Rev.* **1997**, *97*, 637.
(2) Review on [*m.m*]ferrocenophanes: Mueller-Westerhoff, U. T. *Angew. Chem.* **1986**, *98*, 700; *Angew. Chem., Int. Ed. Engl.* **1986**, *25*, 702.
(3) (a) Zechel, D. L.; Foucher, D. A.; Pudelski, J. K.; Yap, G. P. A.; Rheingold, A. L.; Manners, I. *J. Chem. Soc., Dalton Trans.* **1995**, 1893. (b) Clearfield, A.; Simmons, C. J.; Withers, H. P.; Seyferth, D. *Inorg. Chim. Acta* **1983**, *75*, 139. (c) Utri, G.; Schwarzhans, K.-E.; Allmaier, G. M. *Z. Naturforsch.* **1990**, *45b*, 755.
(4) Jutzi, P.; Lenze, N. Neumann, B.; Stammler, H.-G. *Angew. Chem.* **2001**, *113*, 1470; *Angew. Chem., Int. Ed.* **2001**, *40*, 1424.
(5) Uhl, W.; Hahn, I.; Jantschak, A.; Spies, T. *J. Organomet. Chem.* **2001**, *637*−*639*, 300.
(6) Manners, I. *Angew. Chem.* **1996**, *108*, 1712; *Angew. Chem., Int. Ed.* **1996**, *35*, 1602.
(7) Althoff, A.; Jutzi, P.; Lenze, N.; Neumann, B.; Stammler, A.; Stammler, H.-G. *Organometallics* **2002**, *21*, 3018.
(8) (a) Grosche, M.; Herdtweck, E.; Peters, F.; Wagner, M. *Organometallics* **1999**, *18*, 4669. (b) Dinnebier, R. E.; Wagner, M.; Peters, F.; Shankland, K.; David, W. I. F. *Z. Anorg. Allg. Chem.* **2000**, *626*, 1400.

10.1021/om030115m CCC: $25.00
Publication on Web 05/23/2003

Scheme 1. Formation of 2

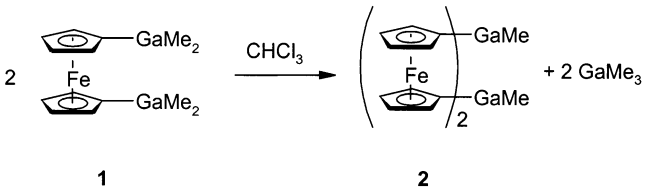

the donor-free digallaferrocenophane **2**. The adducts **2c**,**d**,**f**,**g** possess rodlike polymeric structures in the solid state.

Results

Synthesis and Structure of 2. The donor-free [1.1]-ferrocenophane [{Fe(η^5-C_5H_4)$_2$}$_2${GaMe}$_2$] (**2**) has been synthesized by two slightly different pathways. In the first variant, **2** could be obtained directly from **1** in the form of orange crystals together with trimethylgallium (Scheme 1). This reaction took already place at room temperature, after **1** had been dissolved in trichloromethane. Over the course of 1 week X-ray-quality crystals of **2** formed. In the second variant, **2** was prepared via the diethyl ether adduct **2a** (vide infra), which was formed from 1,1′-bis(dimethylgallyl)ferrocene (**1**) in toluene/diethyl ether solution with concomitant formation of the diethyl ether adduct of trimethylgallium (Scheme 2). This reaction took place at room temperature after **1** had been dissolved in a mixture of toluene and diethyl ether. When dried in vacuo, **2a** decomposed to give **2** in the form of an orange powder. The overall yield of **2** was 46%. Compound **2** is sparingly soluble in nondonor solvents and is air sensitive. It is a thermolabile compound, and heating to 80 °C results in the formation of the trinuclear ferrocenophane [{Fe(C_5H_4)$_2$}$_3$-Ga_2] and trimethylgallium. Therefore, amorphous **2** cannot be transformed into a crystalline material by recrystallization from hot solution. An NMR spectrum was recorded in DMSO-d_6; the spectrum shows data for the DMSO adduct **2e** (Scheme 2).

The structure analysis shows that compound **2** crystallizes in the monoclinic space group $P2_1/n$. Two ferrocene-1,1′-diyl groups are linked together by two GaMe groups with formation of a [1.1]ferrocenophane frame in an anti conformation. Interestingly, only weak van der Waals interactions are observed between the molecular units, so that **2** is regarded as a monomeric species. A drawing of the molecule in the form of a thermal ellipsoid plot is given in Figure 1. Table 1 summarizes selected distances and angles.

The main structural features of **2** are given by the *bridge* (α), the *rotation* (β), the *tilt* (γ), and the *dip* angles (δ) (see Figure 2). These angles in **2** amount to α = 118.60(6)°, β = 14°, γ = 4°, and δ = 5°. The nonbonding Ga−Ga distance is 4.414 Å, and the nonbonding Fe−Fe distance is 5.455 Å. The coordination geometry at the gallium atoms is trigonal planar (angle sum 359°). The Ga(1)−C(1), Ga(1)−C(6A), and Ga−C_{Me} bond distances are typical for gallium organyls.[10] The shortest nonbonding distance between the α-H(Cp) atoms within the ferrocene-1,1′-diyl units is 2.308 Å (r_{vdw} of the H atom ∼1.0 Å). The C(Cp)−Ga bonds are bent *toward* the iron centers with reference to the Cp plane (δ = 5°; see Figure 2). This bonding situation can be compared with that in borylferrocenes,[11] gallylferrocenes,[7] and ferrocenyl carbocations.[12] The smallest dip angle is observed in **2**, thus indicating only weak attractive interactions. Compound **2** reveals structural parameters similar to

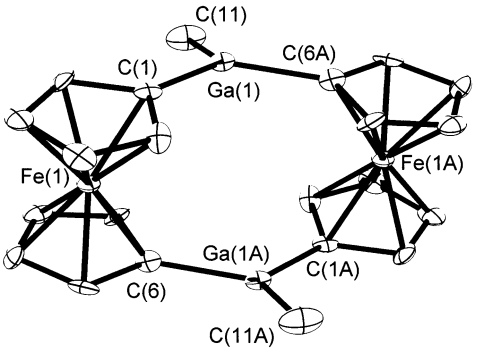

Figure 1. Molecular structure of **2**, with thermal ellipsoids given at the 50% probability level.

Table 1. Selected Distances (Å) and Angles (deg) for 2

	Distances		
Ga(1)−C(1)	1.9442(15)	Ga(1)−Fe(1A)	3.536
Ga(1)−C(6A)	1.9456(15)	Ga−Ga	4.414
Ga(1)−C(11)	1.9502(18)	Fe−Fe	5.455
Ga(1)−Fe(1)	3.481		
	Angles		
C(1)−Ga(1)−C(6A) (α)	118.60(6)	Cp−Cp tilt (γ)	4
C(1)−Ga(1)−C(11)	120.00(8)	dip angle (δ)	5
C(6A)−Ga(1)−C(11)	120.00(8)	∑C−Ga−C	359
Cp−Cp rotation (β)	14		

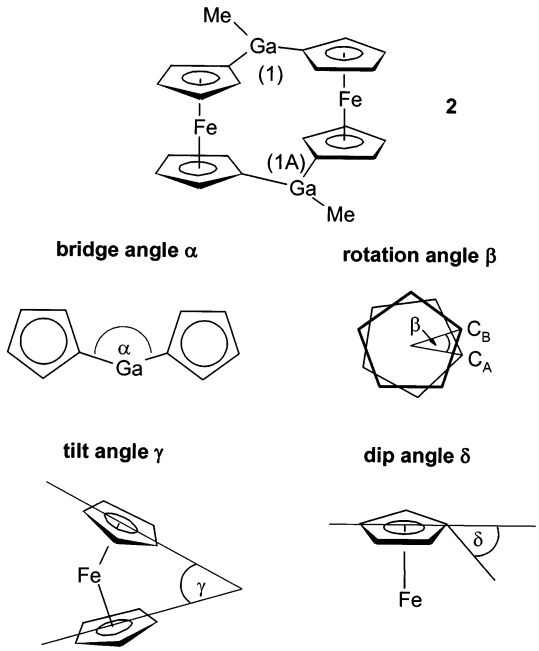

Figure 2. Definition of structural parameters in **2**.

(9) (a) Löwendahl, J.-M.; Håkansson, M. *Organometallics* **1995**, *14*, 4736. (b) Löwendahl, J.-M.; Davidsson, Ö.; Ahlberg, P.; Håkansson, M. *Organometallics* **1993**, *12*, 2417.

(10) Cambridge Crystallographic Structural Database.

(11) (a) Wrackmeyer, B.; Dörfler, U.; Milius, W.; Herberhold, M. *Polyhedron* **1995**, *11*, 1425. (b) Appel, A.; Jäkle, F.; Priemeier, T.; Schmid, R.; Wagner, M. *Organometallics* **1996**, *15*, 1188.

(12) Kreidlin, A. Z.; Dolgushin, F. M.; Yanovsky, A. I.; Kerzina, Z. A.; Petrovskii, P. V.; Rybinskaya, M. I. *J. Organomet. Chem.* **2000**, *616*, 106.

Scheme 2. Formation of Adducts from Donor Molecules and 1 and 2, Respectively

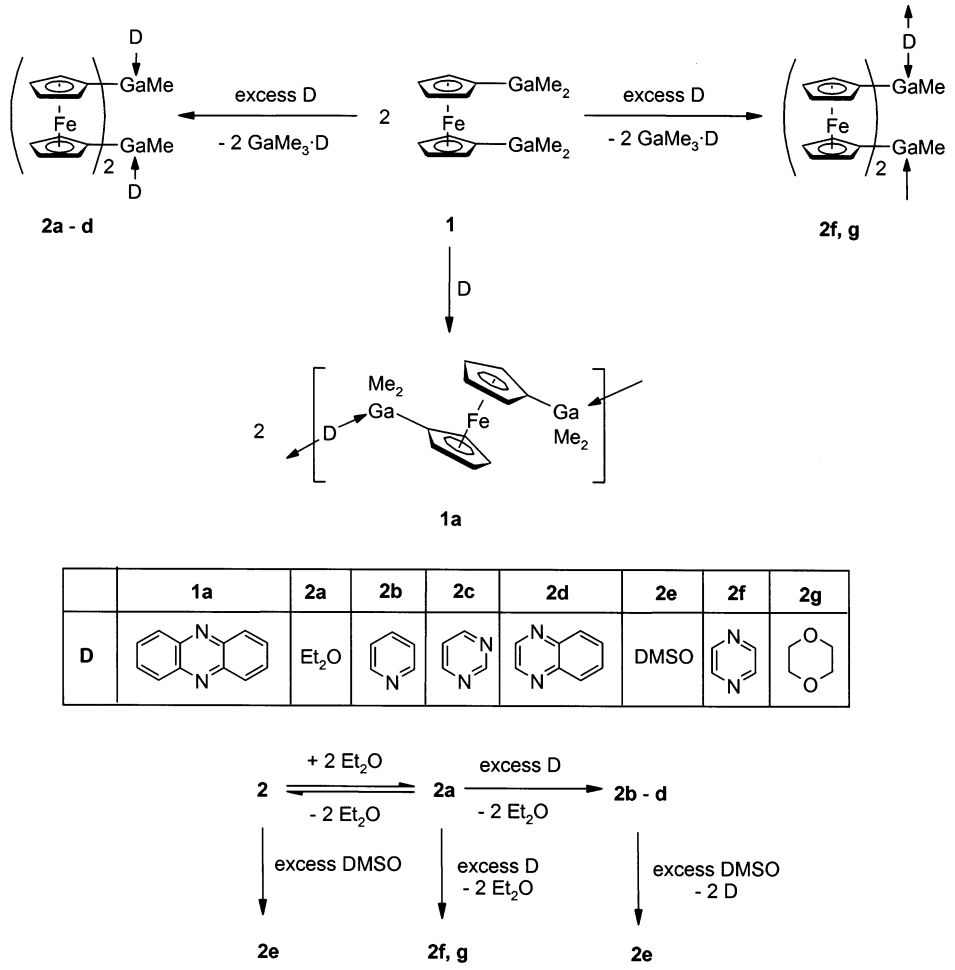

	1a	2a	2b	2c	2d	2e	2f	2g
D		Et_2O				DMSO		

those of the digalla[1.1]ferrocenophane $[\{Fe(C_5H_4)_2\}_2\{GaCH(SiMe_3)_2\}_2]$.[5] The three-coordinate gallium atoms in **2** allow the formation of coordination compounds. In the following, donor−acceptor compounds with quite different association behaviors in the solid state will be described.

Synthesis and Structure of Coordination Compounds [2·2D] (2a−d). As already mentioned, the diethyl ether adduct **2a** could be prepared from **1** and excess diethyl ether (Scheme 2). After the diethyl ether solution was cooled to +6 °C, the adduct **2a** precipitated in the form of air-sensitive orange crystals suitable for X-ray crystal structure analysis. Compound **2a** turned out to be rather thermolabile and decomposes even at room temperature with formation of **2** and diethyl ether. It is sparingly soluble in nondonor solvents.

The coordination compounds **2b−d** have been prepared by two different methods (Scheme 2). The first one starts with the synthesis of **2a** as described above. When aromatic nitrogen donors D were added to **2a**, substitution of the Et_2O molecule immediately took place. The air-sensitive adducts **2b−d** were formed in rather good yields, but no crystals suitable for X-ray diffraction analysis were formed. Recrystallization of **2b−d** turned out to be impossible because of their thermolability. Heating of **2b−d** to 80 °C resulted in the formation of the respective donor-stabilized trinuclear ferrocenophanes $[\{Fe(C_5H_4)_2\}_3\{Ga(D)\}_2]$ and donor adducts of trimethylgallium. Following the second synthetic method, **1** and the donor molecules were treated with toluene and then warmed to 40 °C until a clear solution had formed. After a few days at room temperature the adducts **2b−d** were obtained suitable for X-ray diffraction analysis. The crystals are sparingly soluble in nondonor solvents and also only sparingly soluble in diethyl ether, pyridine, and pyrimidine. This procedure resulted in lower yields than the first one.

The compounds **2a−d** have been characterized using X-ray structure determination, NMR spectroscopy, and elemental analysis. The solubility of **2** and **2a−d** in DMSO stems from the formation of the monomeric adduct **2e**. The NMR spectra were recorded in DMSO-d_6; thus, the spectra show data for the DMSO adduct **2e** and for the free donor molecules.

The diethyl ether complex **2a** crystallizes in the monoclinic space group $P2_1/n$. The compound maintains the anti conformation and the framework parameters of **2**. A drawing of the molecular structure in form of a thermal ellipsoid plot is given in Figure 3. Table 2 summarizes selected distances and angles for **2a−d**. The gallium atoms show an only slightly distorted trigonal pyramidal coordination geometry (C−Ga−C angle sum 355°). In general, the geometry of compounds with tetracoordinated gallium atoms varies between trigonal pyramidal and tetrahedral.[10] Due to the small deviation from planarity at the gallium atoms, the methyl groups are only slightly bent out of the plane of the $GaCp_2$ unit toward the iron centers. The dip angle

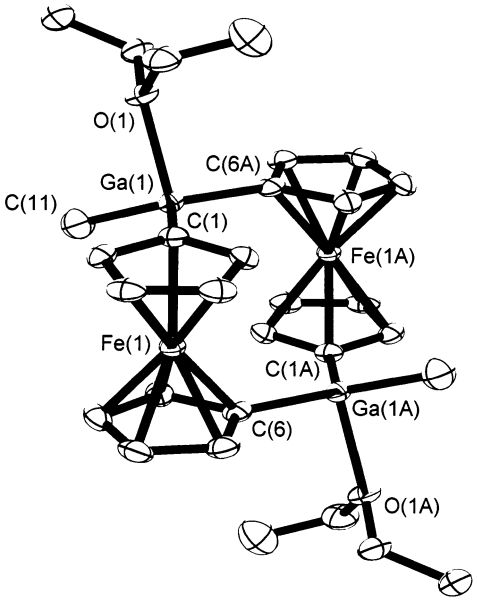

Figure 3. Molecular structure of **2a**, with thermal ellipsoids given at the 50% probability level.

Table 2. Selected Distances (Å) and Angles (deg) for 2a−d

	2a	**2b**	[**2c**·(toluene)]	**2d**
		Distances		
Ga(1)−C(1)	1.962(4)	1.981(6)	1.970(2)	1.9630(19)
Ga(1)−C(6A)	1.957(3)	1.957(6)	1.961(2)	1.965(2)
Ga(1)−C(11)	1.977(4)	1.976(7)	1.976(2)	1.978(2)
Ga(1)−N/O	2.153(2)	2.144(5)	2.1508(16)	2.2192(16)
Ga(1)−Fe(1)	3.618	3.682	3.571	3.626
Ga(1)−Fe(1A)	3.51	3.54	3.608	3.593
Ga−Ga	4.648	4.768	4.631	4.734
Fe−Fe	5.432	5.427	5.485	5.448
donor−donor		3.515(8)	3.528(3)	3.458(3)
		Angles		
C(1)−Ga(1)−C(6A) (α)	116.44(14)	115.6(2)	115.92(9)	116.96(8)
C(1)−Ga(1)−C(11)	121.82(15)	117.9(3)	119.42(11)	115.39(9)
C(6A)−Ga(1)−C(11)	116.64(16)	118.3(3)	117.69(11)	120.44(9)
N/O−Ga(1)−C(1)	97.60(10)	97.5(2)	97.10(7)	95.49(7)
N/O−Ga(1)−C(6A)	97.56(11)	100.0(2)	97.88(7)	97.20(7)
N/O−Ga(1)−C(11)	97.48(14)	101.2(2)	101.49(8)	104.17(8)
Cp−Cp rotation (β)	9	10	9	10
Cp−Cp tilt (γ)	2	3	1	2
dip angle (δ)	3	1	2	0
ΣC−Ga−C	355	352	353	353

is $\delta = 3°$, thus indicating only weak Fe−Ga interactions. The ether molecules are coordinated in the axial position.

The pyridine complex **2b** crystallizes in the monoclinic space group *C*2/*c* (Figure 4). The Ga−C_{Me} bond distances are comparable to those found in **2**. The Ga−N bond distances of 2.144(5) Å are typical for donor−acceptor adducts formed from sp^2-nitrogen donors and three-coordinated gallium acceptors.[10] The C−Ga−C angle sum at each gallium atom is 352° and thus shows a slightly more pronounced distortion than in **2a**. The pyridine molecules are coordinated in the axial position. Complex **2b** is regarded as a polymeric compound which consists of [**2**·2(pyridine)] units (see Figure 4). Each polymer strand is surrounded by six other strands and aligned parallel to the crystallographic *a*−*c* diagonal. The molecular units are linked by π-stacking interactions between the pyridine molecules. The distance between the aromatic rings is 3.515 Å, which is typical for weak interactions.[10] The solid-state structure of uncoordinated pyridine reveals no π-stacking interactions.[13]

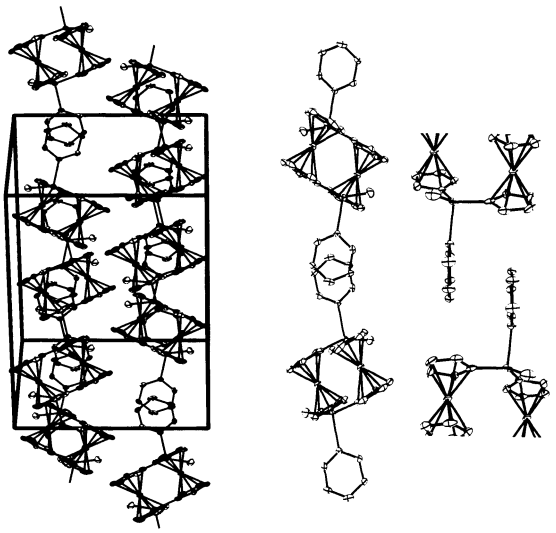

Figure 4. Solid-state structure of **2b**, including the unit cell. A drawing of two molecular units of **2b** is shown on the right side (two different views).

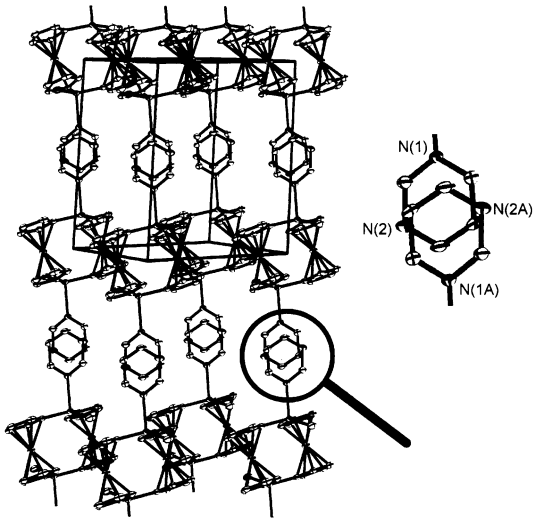

Figure 5. Solid-state structure of [**2c**·(toluene)], including the unit cell (the disordered toluene molecules are not shown). The π-stacking between two pyrimidine rings is shown in more detail on the right side of the picture.

The pyrimidine complex **2c** crystallizes as [**2c**·(toluene)] in the triclinic space group $P\bar{1}$ (Figure 5). It shows a disorder of toluene molecules located at an inversion center. The [**2**·2(pyrimidine)] unit reveals structural parameters similar to those of the [**2**·2(pyridine)] unit. [**2c**·(toluene)] shows Ga−N bonds (2.1508(16) Å) only slightly longer than those found in **2b** (2.144(5) Å). The molecular units of [**2c**·(toluene)] form polymer strands in a manner similar to that for **2b**. They are aligned parallel to the crystallographic *c* axis. A distance of 3.528 Å between the pyrimidine planes is observed. Regarding the position of the pyrimidine molecules, the N atoms are arranged with the greatest possible distance. The solid-state structure of uncoor-

(13) Mootz, D.; Wussw, H.-G. *J. Chem. Phys.* **1981**, *75*, 1517.

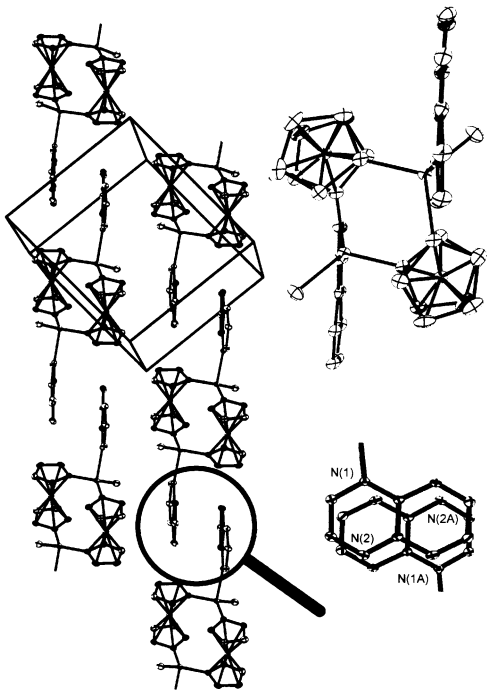

Figure 6. Solid-state structure of **2d**, including the unit cell. The π-stacking between two quinoxaline rings is shown in more detail on the right side of the picture. A drawing of one molecular unit of **2d**, viewed along the crystallographic $b-c$ diagonal, is shown in the upper right corner.

dinated pyrimidine reveals the N atoms stacked upon each other with a distance of 3.806 Å between the ring planes.[14] Accordingly, there are stronger π-stacking interactions in [**2c**·(toluene)] than in uncoordinated pyrimidine. It could be expected that **2** would react with pyrimidine to give the polymeric coordination compound [**2**·(pyrimidine)] (using both nitrogen atoms as donors). Instead, the formation of [**2c**·(toluene)] was observed. Even a reaction in a 1:1 stoichiometry did not result in the formation of [**2**·(pyrimidine)].

The quinoxaline complex **2d** crystallizes in the triclinic space group $P\bar{1}$ (Figure 6). The molecular unit reveals structural parameters similar to that of the [**2**·(pyrimidine)] unit. It is evident from the orientation of the quinoxaline ligands that the annelated benzene ring in the quinoxaline molecule is directed away from the ferrocenophane fragment. The structure of **2d** consists of polymer strands similar to those of **2b** and [**2c**·(toluene)]. They are aligned parallel to the crystallographic $b-c$ diagonal. The distance between the aromatic rings is 3.458 Å and is thus shorter than in **2b** and [**2c**·(toluene)]. The solid-state structure of uncoordinated quinoxaline reveals π-stacking interactions with the nitrogen-containing rings positioned on top of each other, while the rings in **2d** are twisted by 180°, resulting in a displacement of the ferrocenophane compared to the orientation in **2c**. The distance between the aromatic rings is 3.901 Å in uncoordinated quinoxaline, thus indicating weaker π-stacking interactions than in **2d**.[15] Similar to the situation with pyrimidine as donor, the formation of the coordination polymer [**2**·(quinoxaline)] using both nitrogen donors in quinoxaline seemed possible. Instead, **2d** was formed, even when a 1:1 stoichiometry of the reactants was applied.

Table 3. Selected Distances (Å) and Angles (deg) for 2f,g

	[**2f**·1.5(pyrazine)·1.5(toluene)]	**2g**
	Distances	
Ga(1)−C(1)	1.9605(17)	1.955(2)
Ga(1)−C(6A)	1.9656(17)	1.961(3)
Ga(1)−C(11)	1.9775(19)	1.986(3)
Ga(1)−N/O	2.1854(14)	2.2000(17)
Ga(1)−Fe(1)	3.612	3.457
Ga(1)−Fe(1A)	3.541	3.595
Ga−Ga	4.637	4.476
Fe−Fe	5.448	5.451
	Angles	
C(1)−Ga(1)−C(6A) (α)	116.10(7)	117.81(11)
C(1)−Ga(1)−C(11)	116.69(8)	117.31(11)
C(6A)−Ga(1)−C(11)	121.03(8)	120.73(11)
N/O−Ga(1)−C(1)	98.80(6)	97.31(8)
N/O−Ga(1)−C(6A)	96.54(6)	96.31(8)
N/O−Ga(1)−C(11)	99.62(7)	96.78(10)
Cp−Cp rotation (β)	9	11
Cp−Cp tilt (γ)	1	3
dip angle (δ)	3	5
$\sum$C−Ga−C	354	356

Synthesis and Structure of Coordination Compounds [2·D] (2f,g). Coordination compounds of the type [**2**·D] were prepared using the same two methods as described above for the coordination compounds **2b**−**d**. The adducts **2f**,**g**, with pyrazine (**2f**) and dioxane (**2g**) as donors, are only sparingly soluble in donor and nondonor solvents. They have been characterized by X-ray structure and elemental analysis. Selected bond lengths and bond angles of **2f**,**g** are given in Table 3. Solution NMR spectra could not be measured, due to their low solubility at room temperature even in donor solvents. Gentle warming resulted in thermal decomposition with formation of the donor-stabilized trinuclear ferrocenophanes [{Fe(C_5H_4)$_2$}$_3${Ga(D)}$_2$] and the donor adducts of trimethylgallium.

The pyrazine complex **2f** crystallizes as [**2f**·1.5(pyrazine)·1.5(toluene)] in the triclinc space group $P\bar{1}$ (Figure 7). The crystals show a disorder of pyrazine and toluene molecules. The Ga−N bond distances are 2.1854(14) Å. The compound consists of polymer strands aligned parallel to the crystallographic $a-b-c$ diagonal. The ferrocenophane molecules form sheets with all units of **2** arranged parallel to the similar units of the neighbored strands; the shortest intramolecular Fe−Fe distance is 5.448 Å, and the shortest intermolecular Fe−Fe distance is 5.609 Å. The sheets alternate with layers of the pyrazine donors containing also the disordered toluene and pyrazine molecules. The pyrazine ring planes are not arranged parallel to each other, so that π-stacking interactions between the pyrazine rings cannot arise.

The dioxane complex **2g** crystallizes in the monoclinic space group $P2_1/c$ (Figure 8). The Ga−O bond distances are slightly longer than those found in **2a**. The dioxane donors are fixed in a chair conformation. Regarding the dip angle ($\delta = -5°$), a bending *toward* the Fe atoms is observed, as described for [**2f**·1.5(pyrazine)·1.5(toluene)]. Similar to [**2f**·1.5(pyrazine)·1.5(toluene)], **2g** consists of

(14) Wheatley, P. J. *Acta Crystallogr.* **1960**, *13*, 80.
(15) Anthony, A.; Desiraju, G. R.; Jetti, R. K. R.; Kuduva, S. S.; Madhavi, N. N. L.; Nangia, A.; Thaimattam, R.; Thalladi, V. R. *Cryst. Eng.* **1998**, *1*, 1.

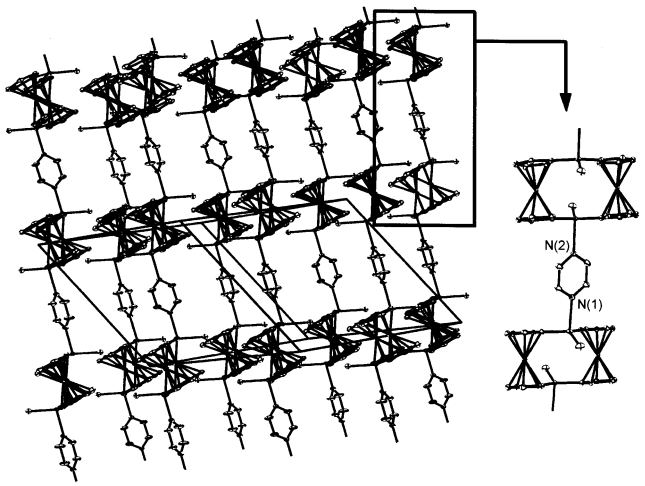

Figure 7. Solid-state structure of [**2f**·1.5(pyrazine)·1.5-(toluene)], including the unit cell (the disordered pyrazine and toluene molecules are not shown). The bonding situation between the ferrocenophane and pyrazine is shown in more detail on the right side of the picture.

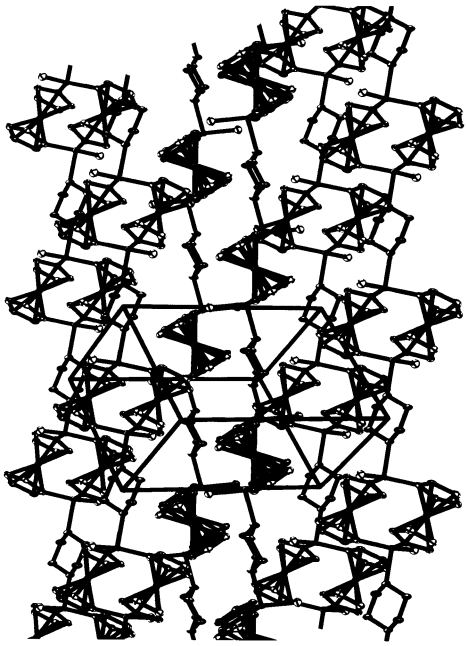

Figure 8. Solid-state structure of **2g**, including the unit cell.

polymer strands. They are aligned parallel to the crystallographic *a*−*c* diagonal.

Reaction of 1 and 2 with Phenazine. The reaction of **1** with phenazine did not result in the formation of [**2**·2(phenazine)], even after prolonged heating. Instead, the coordination polymer [**1**·(phenazine)] **1a** was formed as green crystals (Scheme 2). We have reported the preparation and the solid-state structure of **1a** in a previous publication.[7] With regard to the observation described above, it is not surprising that **2a** also does not react with phenazine.

Dynamic Behavior of 2e in Solution. The ^{1}H NMR spectrum of a solution of **2e** in DMSO-d_6 displays one signal for all α-CH units and one signal for all β-CH units of the ferrocene-1,1′-diyl fragments. This observation indicates an averaged, highly symmetrical structure in solution with equilibrating anti and syn conformations. A comparable dynamic behavior has been observed for the *Sn,Sn*′-tetra-*n*-butyldistanna[1.1]ferrocenophane, also possessing an anti conformation in the solid state.[2,3b] In contrast, the more rigid carbon-bridged compound *exo,exo,anti*-1,12-dimethyl[1.1]ferrocenophane displays four ^{1}H NMR signals, two signals for the α-CH units and two signals for the β-CH units of the ferrocene-1,1′-diyl fragments.[9b] The dynamic behavior of [1.1]ferrocenophanes in solution has been already discussed in more detail, including a proposal for an *anti-twist-syn*-transfer mechanism.[2,9a]

Table 4. UV/Vis Spectroscopic Data

compd	λ_{max} (nm)	compd	λ_{max} (nm)
2	466	**2f**	518
2b	482	**2g**	469
2c	464	ferrocene	469
2d	549		

Electrochemistry of 2b. A cyclic voltammogram of **2b** was recorded using pyridine as solvent and tetrabutylammonium fluoride (TBAPF) as the supporting electrolyte.[16] Reversible oxidation potentials are observed at $E_{1/2}(1) = -314$ mV and $E_{1/2}(2) = -114$ mV (versus ferrocene/ferrocenium), with a peak separation of 90 mV. The difference in the oxidation potentials ($\Delta E_{1/2} =$ 200 mV) indicates only a partial electron delocalization in the cationic species (presumably, class II in the Robin and Day classification[1]). In Figure 9, the first oxidation potentials of ferrocene and decamethylferrocene are compared with those of boron- and gallium-substituted ferrocenes, measured in pyridine as solvent. The lowest potential is observed for $Fe(C_5Me_5)_2$. The electron-donating ability decreases in the order $Fe(C_5Me_5)_2$ > $Fe(C_5H_4BMe_2{\cdot}Py)_2$[7] > $Fe(C_5H_4GaMe_2{\cdot}Py)_2$] (**1**·2Py)[7] > $Fe\{[GaMe(Py)H_4C_5]_2Fe\}$ (**2b**).

Mass Spectrometry of 2 and 2b−d,f,g. In the mass spectrum of **2**, the peak of the molecular ion $\mathbf{2}^+$ was not observed; interestingly, the molecular ion of the condensation product $[\{Fe(C_5H_4)_2\}_3Ga_2]^+$ could be detected. Similarly, in the spectra of the coordination complexes **2b**−**d**,**f**,**g**, peaks for the molecular ions [**2**·2D]$^+$, [**2**·D]$^+$, and $\mathbf{2}^+$ were not observed; again, the molecular ion of the condensation product $[\{Fe(C_5H_4)_2\}_3Ga_2]^+$ could be found. Thus, condensation reactions take place very easily under mass spectrometric conditions. A comparable behavior has been described for **1**;[7] the $[\{Fe(C_5H_4)_2\}_3Ga_2]^+$ peak but not the $\mathbf{1}^+$ peak could be detected.

UV/Vis Spectroscopy of 2 and 2b−d,f,g. UV/vis spectroscopic data for **2** and its adducts **2b**−**d**,**f**,**g** in the solid state are given in Table 4. The compounds **2** and **2b**,**c**,**g** exhibit a yellow to orange color (λ_{max} 464−482 nm); only small differences in the spectra can be observed. Compounds **2d** (λ_{max} 549 nm) and **2f** (λ_{max} 518 nm) exhibit an intense purple color, and single crystals of these compounds are almost black. The observed absorptions can be attributed mainly to internal transitions within the molecular units. One may assume electron delocalization to occur between molecular units along the polymer chains of the coordination compounds **2d**,**f**, but this assumption is not supported by band structure calculations.

(16) A solution of **2b** in pyridine was prepared by dissolving **2** in pyridine. Compound **2b** is insoluble in pyridine at room temperature. Heating results in the formation of $[\{Fe(C_5H_4)_2\}_3\{Ga(pyridine)\}_2]$ and the pyridine adduct of trimethylgallium.

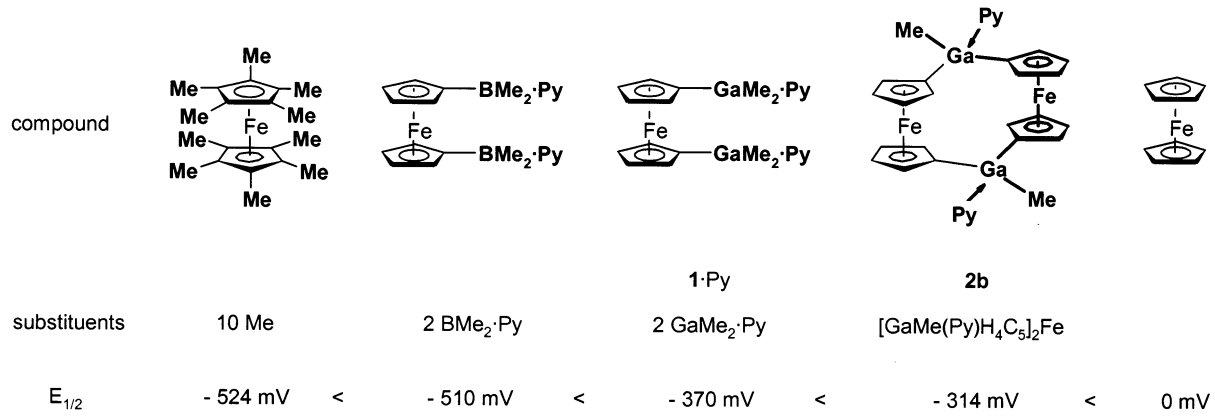

Figure 9. First oxidation potentials (in pyridine) of substituted ferrocenes (functional groups given in boldface letters).

Reversibility of Ferrocenophane Formation. We have reported that the ferrocenophane **2** can be prepared in quantitative yield by elimination of trimethylgallium from the 1,1′-bis(dimethylgallyl)ferrocene **1**. Similarly, the adducts of **2** can be synthesized by starting from **1** and the corresponding donor. In separate experiments we could demonstrate that also the reverse reactions are feasible. Thus, **2** reacts with excess trimethylgallium at 100 °C in a closed flask with quantitative formation of **1**. Similarly the compounds **2a**−**d**,**f**,**g** react with excess trimethylgallium to give of **1** and the donor adduct of trimethylgallium. The reversibility of the formation of **2** is described in eq 1.

$$2\,\mathbf{1} \rightleftharpoons \mathbf{2} + 2GaMe_3 \qquad (1)$$

Discussion

A novel route to [1.1]ferrocenophanes has been found, with the synthesis of the gallium-bridged ferrocenophane [{Fe(C_5H_4)$_2$}$_2${GaMe}$_2$] (**2**) and of its donor adducts **2a**−**g**. The synthetic strategy depends on rather labile ferrocenyl−gallium and methyl−gallium bonds, so that substituent exchange reactions can take place easily. Thus, gentle warming of Fe($C_5H_4GaMe_2$)$_2$ (**1**) leads, with elimination of trimethylgallium in quantitative yields, to the formation of **2**. Donor adducts of **2** are formed under comparable conditions. Interestingly, **2** can be transferred back to **1** in the presence of trimethylgallium. The equilibrium situation as described in eq 1 is characterized by only small enthalpy differences; the number of Ga−C bonds is the same on both sides, and the Ga−ferrocenyl and the Ga−methyl bond strengths are regarded as comparable. Entropic factors shift the equilibrium to the right side.

The lability of the Ga−C bonds in substrates and products is caused by the easy formation of dimeric transition state complexes in exchange reactions. The coordinative unsaturation of the gallium atoms allows the formation of electron-deficient bonds in dimeric units. In the ground-state structure of **1**, weakly bonded dimers with methyl groups in bridging positions are observed (see the solid-state structure of **1**[7]). In transition-state structures necessary for exchange reactions, ferrocenyl groups also have to be placed in bridging positions.

Highly stereo- and regiospecific substitution reactions are necessary to transform **1** into **2**. The reversibility as described in eq 1 allows the correction of mistakes concerning the specifity of exchange reactions ("proofreading" process[17]). In general, reversibility is a prerequisite for reactions performed under the concept of "dynamic covalent chemistry".[17]

The dynamic structure of **2** and of its adducts in solution is based on fast rearrangements between syn and anti conformations of the ferrocenophane fragments and on fast coordination/decoordination processes of the respective donor molecules. In the solid state, these compounds are present in the anti conformation with the donor molecules in an axial position.

Several rodlike polymeric coordination compounds possessing a digalla[1.1]ferrocenophane as a molecular building block could be prepared (**2b**−**d**,**f**,**g**) and structurally characterized. These polymers are formed independent from the stoichiometry of the reactants. Two bonding situations have been observed for the bridging difunctional donor units: (i) Difunctional donors such as pyrazine and dioxane act, as expected, as bidentate ligands (formation of **2f**,**g**), (ii) bidentate ligand pairs are formed by π-stacking interactions between mono- and difunctional donors such as pyridine, pyrimidine, and quinoxaline (formation of **2b**−**d**). The coordination modes of the donor molecules in **2b**−**d**,**f**,**g** are presented in Figure 10. Steric reasons might prevent the function of pyrimidine as a bidentate donor. The reason quinoxaline does not act as a bidentate donor is not obvious.

It is interesting to regard in more detail the coordination behavior of pyrazine and its benzannelated derivatives quinoxaline and phenazine. No steric hindrance between pyrazine and the ferrocenophane framework and, thus, a free rotation around the Ga−N bond without any restrictions concerning possible conformations is observed in complex **2f**. However, the quinoxaline donor molecules of complex **2d** show a special conformation, with an orientation of the annelated benzene ring directed away from the Cp rings of the ferrocenophane unit (see Figure 6). This observation is an indication for steric repulsion as a structure-directing factor. This conclusion is strongly supported by the coordination behavior of the bidentate donor phenazine, possessing two annelated benzene rings. Due to steric reasons, this compound does not react with the ferro-

(17) Review on dynamic covalent chemistry: Rowan, S. J.; Cantrill, S. J.; Cousins, G. R. L.; Sanders, J. K. M.; Stoddart, J. F. *Angew. Chem.* **2002**, *114*, 938; *Angew. Chem., Int. Ed.* **2002**, *41*, 898.

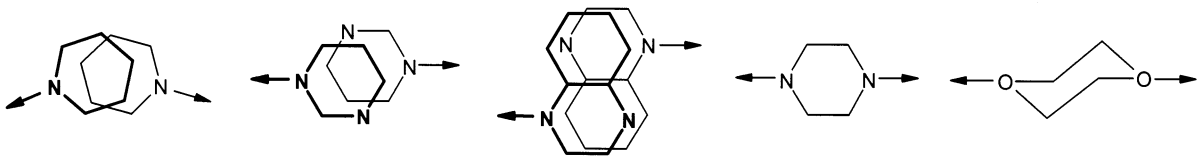

Figure 10. Coordination modes of the donor molecules in **2b**−**d**,**f**,**g** (the π electrons of the aromatic nitrogen donors are not shown).

cenophane **2**. As expected, it reacts with 1,1′-bis(dimethylgallyl)ferrocene (**1**).[7]

The ferrocenophane **2** turns out to be an interesting building block in supramolecular chemistry. We are currently trying to prepare suitably substituted digallaferrocenophanes with the aim of preparing better soluble coordination polymers.

Experimental Section

General Comments. All manipulations were carried out under a purified argon atmosphere using standard Schlenk techniques. The solvents were commercially available, purified by conventional means, and distilled immediately prior to use. The NMR spectra were recorded in DMSO-d_6 using a Bruker Advance DRX 500 spectrometer (^{1}H, 500.1 MHz). Chemical shifts are reported in ppm and were referenced to the solvent resonances as an internal standard. The elemental analyses were performed by the Microanalytical Laboratory of the Universität Bielefeld. Cyclic voltammograms were recorded on an EG&G potentiostat, Model 273A, controlled by M 250/270 software. The solvent was pyridine, and the supporting electrolyte was tetrabutylammonium fluoride (TBAPF), which was purchased from Fluka and used without further purification. The electrolyte concentration was 0.1 M. The voltammetric measurements were performed using a platinum-disk electrode (d = 2 mm), which was polished prior to use. Potentials were calibrated by the method of Gagné and are quoted vs the ferrocenium−ferrocene couple as an internal standard.[18] A platinum wire was used as a counter electrode. UV−vis data were collected using a Shimadzu UV-3101PC spectrometer (250−800 nm). The samples were measured as barium sulfate triturates for solid-state reflection spectroscopy.

Starting Materials. 1,1′-Bis(dimethylgallyl)ferrocene (**1**) was prepared using a literature procedure.[7]

Preparation of 2. (a) In a Schlenk flask (25 mL) **1** (300 mg, 0.78 mmol) was treated with diethyl ether (1 mL) and toluene (3 mL) at room temperature. Then the reaction mixture was cooled to +6 °C. After 1 day an orange, crystalline solid had formed, which was washed with *n*-hexane and dried in vacuo to give 98 mg (0.18 mmol, 46%) of **2**.

(b) In an NMR tube **1** (35 mg, 0.09 mmol) was dissolved in trichloromethane. The solution was cooled to +6 °C. After 1 week, single X-ray-quality crystals had formed. UV: λ 258, 466 nm. ^{1}H NMR (DMSO-d_6): δ −0.17 (s, 6 H, CH_3), 4.05 (s, 8 H, ring C2/5-H or C3/4-H), 4.18 (s, 8 H, ring C2/5-H or C3/4-H). Anal. Calcd for $C_{22}H_{22}Fe_2Ga_2$ (M_r = 537.54): C, 49.16; H, 4.13. Found: C, 49.04; H, 4.05.

Preparation of 2a. In an NMR tube **1** (35 mg, 0.09 mmol) was treated with diethyl ether (0.2 mL) and toluene (0.7 mL) at room temperature. The resulting solution was cooled to +6 °C. After 1 day orange X-ray-quality crystals of **2a** had formed, which are thermolabile and decomposed even at room temperature. ^{1}H NMR (DMSO-d_6): δ −0.18 (s, 6 H, CH_3), 1.08 (t, ^3J = 6.9 Hz, 12 H, Et_2O CH_3), 3.37 (q, ^3J = 6.9 Hz, 8 H, Et_2O CH_2), 4.03 (s, 8 H, ring C2/5-H or C3/4-H), 4.17 (s, 8 H, ring C2/5-H or C3/4-H).[19]

Preparation of 2b−d,f,g. (a) In a Schlenk flask (25 mL), **1** (300 mg, 0.78 mmol) was treated with diethyl ether (1 mL) and toluene (3 mL) at room temperature. To the resulting solution was added a solution of the donor (2 mmol) in toluene (0.5 mL). After a short time a microcrystalline solid was formed. The solid was washed with *n*-hexane and dried in vacuo. All yields are reported according to this procedure.

(b) In an NMR tube **1** (35 mg, 0.09 mmol) and the donor (0.5 mmol) were dissolved in toluene (0.7 mL) by gentle heating (maximum 40 °C). Single X-ray-quality crystals had grown after 1 day.

2b. Yield: 170 mg (0.24 mmol, 61%). UV: λ 260, 482 nm. ^{1}H NMR (DMSO-d_6): δ −0.17 (s, 6 H, CH_3), 4.05 (s, 8 H, ring C2/5-H or C3/4-H), 4.18 (s, 8 H, ring C2/5-H or C3/4-H), 7.38 (s, 4 H, pyridine), 7.78 (s, 2 H, pyridine), 8.55 (s, 4 H, pyridine). Anal. Calcd for $C_{32}H_{32}Fe_2Ga_2N_2$ (M_r = 695.76): C, 55.24; H, 4.64; N, 4.03. Found: C, 55.58; H, 4.70; N, 4.09. CV: $E_{1/2}(1)$ = −314 mV, $E_{1/2}(2)$ = −114 mV (peak separation 90 mV).

2c. Yield: 176 mg (0.25 mmol, 64%). UV: λ 259, 464 nm. ^{1}H NMR (DMSO-d_6): δ −0.17 (s, 6 H, CH_3), 4.05 (s, 8 H, ring C2/5-H or C3/4-H), 4.18 (s, 8 H, ring C2/5-H or C3/4-H), 7.54 (s, 2 H, pyrimidine), 8.82 (s, 4 H, pyrimidine), 9.20 (s, 2 H, pyrimidine). Anal. Calcd for $C_{30}H_{30}Fe_2Ga_2N_4$ (M_r = 697.73): C, 51.64; H, 4.33; N, 8.03. Found: C, 51.45; H, 4.46; N, 8.06.[20]

2d. Yield: 207 mg (0.26 mmol, 67%) of **2d**. UV: λ 256, 549 nm. ^{1}H NMR (DMSO-d_6): δ −0.18 (s, 6 H, CH_3), 4.04 (s, 8 H, ring C2/5-H or C3/4-H), 4.17 (s, 8 H, ring C2/5-H or C3/4-H), 7.87 (dd, ^4J = 3.1 Hz, ^3J = 6.1 Hz, 4 H, quinoxaline), 8.11 (dd, ^4J = 3.1 Hz, ^3J = 6.1 Hz, 4 H, quinoxaline), 8.96 (s, 4 H, quinoxaline). Anal. Calcd for $C_{38}H_{34}Fe_2Ga_2N_4$ (M_r = 797.86): C, 57.21; H, 4.30; N, 7.02. Found: C, 57.05; H, 4.31; N, 6.81.

2f. Yield: 179 mg (0.29 mmol; 74%). UV: λ 261, 519 nm. Anal. Calcd for $C_{26}H_{26}N_2Fe_2Ga_2$ (M_r = 617.65): C, 50.56; H, 4.24; N, 4.54. Found: C, 50.36; H, 4.26; N, 4.30.[21]

2g. Yield: 168 mg (0.27 mmol; 69%). UV: λ 256, 469 nm. Anal. Calcd for $C_{26}H_{30}Fe_2Ga_2O_2$ (M_r = 625.66): C, 49.91; H, 4.83. Found: C, 49.69; H, 4.68.

Reaction of 2 and 2b−d,f,g with Trimethylgallium. Trimethylgallium ((pyrophoric!) 0.10 g, 0.9 mmol) was added to a suspension of **2** (40 mg, 0.07 mmol) in toluene-d_8 (0.5 mL) in a NMR tube. The reaction mixture was heated to 100 °C in the tightly closed flask until all components had dissolved. When the mixture was cooled to room temperature, **1** formed as an orange microcrystalline solid. The supernatant solution was decanted, and the solid residue was washed with hexane. It was identified using NMR spectroscopy. Only $GaMe_3$ could be identified in the reaction mixture by NMR spectroscopy.

(18) Gagné, R. R.; Koval, C. A.; Lisensky, G. C. *Inorg. Chem.* **1980**, *19*, 2854.

(19) A single crystal was coated with a layer of hydrocarbon oil, attached to a glass fiber, and cooled to 173 K for X-ray structure determination. Because of the thermolability of **2a** no elemental analysis could be performed.

(20) Using method B single crystals of [**2c**·(toluene)] were obtained. When the solvent was removed in vacuo, the crystals decomposed to a yellow powder.

(21) Using method B, single crystals of [**2f**·1.5(pyrazine)·1.5(toluene)] were obtained. When pyrazine and toluene were removed in vacuo, the crystals decomposed to a dark red powder.

The coordination compounds **2b**−**d**,**f**,**g** react with trimethylgallium in a similar manner. The donor adduct of $GaMe_3$ and uncoordinated $GaMe_3$ could be identified in the reaction mixture.

Acknowledgment. The support of this work by the Deutsche Forschungsgemeinschaft, the Universität Bielefeld, and the Fonds der Chemischen Industrie is gratefully acknowledged. We thank Professor Lorberth, University of Marburg, for a gift of trimethylgallium and Professor Müller, University of Bielefeld, for recording the UV/vis spectra.

Supporting Information Available: Tables of crystal data, positional and thermal parameters, and bond lengths and angles. This material is available free of charge via the Internet at http://pubs.acs.org.

OM030115M